GA–A22461

CONF-960919--2

DIVERTOR PLASMA STUDIES ON DIII–D: EXPERIMENT AND MODELING

by

W.P. WEST, S.L. ALLEN, N.H. BROOKS, D.A. BUCHENAUER, T.N. CARLSTROM, J.W. CUTHBERTSON, E.J. DOYLE, T.E. EVANS, M.E. FENSTERMACHER, D.N. HILL, A.W. HYATT, R.C. ISLER, G.L. JACKSON, R. JONG, C.C. KLEPPER, C.J. LASNIER, A.W. LEONARD, M.A. MAHDAVI, R. MAINGI, G.R. MCKEE, W.H. MEYER, R.A. MOYER, D.G. NILSON, T.W. PETRIE, G.D. PORTER, T.L. RHODES, M.J. SCHAFFER, R.D. STAMBAUGH, D.M. THOMAS, S. TUGARINOV, M.R. WADE, J.G. WATKINS, D.G. WHYTE, and R.D. WOOD

SEPTEMBER 1996

GENERAL ATOMICS

DISCLAIMER

GA-A22461

DIVERTOR PLASMA STUDIES ON DIII-D: EXPERIMENT AND MODELING

by
W.P. WEST, S.L. ALLEN,* N.H. BROOKS, D.A. BUCHENAUER,†
T.N. CARLSTROM, J.W. CUTHBERTSON,‡ E.J. DOYLE,△ T.E. EVANS,
M.E. FENSTERMACHER,* D.N. HILL,* A.W. HYATT, R.C. ISLER,◊
G.L. JACKSON, R. JONG,* C.C. KLEPPER,◊ C.J. LASNIER,*
A.W. LEONARD, M.A. MAHDAVI, R. MAINGI,# G.R. MCKEE, W.H. MEYER,*
R.A. MOYER,‡ D.G. NILSON,* T.W. PETRIE, G.D. PORTER,* T.L. RHODES,△
M.J. SCHAFFER, R.D. STAMBAUGH, D.M. THOMAS, S. TUGARINOV,¶
M.R. WADE,◊ J.G. WATKINS,† D.G. WHYTE,∞ and R.D. WOOD*

This is a preprint of a paper to be presented at the Eighth International Conference on Plasma Physics, September 9–11, 1996, Nagoya, Japan, and to be published in *The Proceedings.*

*Lawrence Livermore National Laboratory, Livermore, California.
†Sandia National Laboratory, Livermore, California.
‡University of California, San Diego, California.
△University of California, Los Angeles, California.
◊Oak Ridge National Laboratory, Oak Ridge, Tennessee.
#Oak Ridge Associated Universities Oak Ridge, Tennessee.
¶TRINITI Laboratory, Troitsk, Moscow Region.
∞INRS — Energie et Materiaux, Varennes, Quebec, Canada.

Work supported by
the U.S. Department of Energy
under Contract Nos. DE-AC03-89ER51114, W-7405-ENG-48,
DE-AC04-94AL85000, DE-AC05-96OR22464, and Grant Nos.
DE-FG03-86ER53266 and DE-FG03-95ER54294

GA PROJECT 3466
SEPTEMBER 1996

ABSTRACT

In a magnetically diverted tokamak, the scrape-off layer (SOL) and divertor plasma provides separation between the first wall and the core plasma, intercepting impurities generated at the wall before they reach the core plasma. The divertor plasma can also serve to spread the heat and particle flux over a large area of divertor structure wall using impurity radiation and neutral charge exchange, thus reducing peak heat and particle fluxes at the divertor strike plate. Such a reduction will be required in the next generation of tokamaks, for without it, the divertor engineering requirements are very demanding. To successfully demonstrate a radiative divertor, a highly radiative condition with significant volume recombination must be achieved in the divertor, while maintaining a low impurity content in the core plasma.

Divertor plasma properties are determined by a complex interaction of classical parallel transport, anomalous perpendicular transport, impurity transport and radiation, and plasma wall interaction. In this paper we will describe a set of experiments on DIII–D designed to provide detailed two dimensional documentation of the divertor and SOL plasma. Measurements have been made in operating modes where the plasma is attached to the divertor strike plate and in highly radiating cases where the plasma is detached from the divertor strike plate. We will also discuss the results of experiments designed to influence the distribution of impurities in the plasma using enhanced SOL plasma flow. Extensive modeling efforts will be described which are successfully reproducing attached plasma conditions and are helping to elucidate the important plasma and atomic physics involved in the detachment process.

1. INTRODUCTION

It has long been recognized that the plasma/wall interaction in a magnetically confined fusion plasma can have a deleterious effect on plasma performance. Much effort has been put on improving wall conditions and modifying the magnetic topology to reduce the influence of the wall. In the early 80's, several tokamaks conducted experiments designed to test the performance of a poloidally diverted configuration. The success, most notably the achievement of the H-mode, i.e. the High Confinement Mode, in ASDEX [1] during high power neutral beam injection, led to a new generation of diverted tokamak experiments. During the following decade the success of diverted tokamaks, such as JET, JT-60U, ASDEX Upgrade, and DIII-D, has been remarkable..

A cross section of a diverted DIII–D plasma including flux surface contours is shown in Fig. 1. The poloidal divertor serves to magnetically isolate the region of strong plasma/wall interaction from the confined core plasma. This isolation helps to reduce the flux of recycled fuel particles and sputtered wall impurities back to the core, thus helping to maintain plasma density control and cleanliness. In addition, the divertor configuration helps to spread the heat and particle flux emanating from the core plasma over the entire footprint of the divertor strike point, avoiding the localized very high heat flux frequently observed on discrete limiter tokamaks. The divertor thus reduces the likelyhood of such disasterous events as runaway wall material sublimation. The configuration can also be used to efficiently conduct helium ash to exhaust pumps. Despite the fact that these advantages come at a high price, requiring additional plasma shaping coils and consuming a significant fraction of the volume of the confinement vessel, the designs for all of the next generation of tokamaks, such as ITER, have included poloidal divertors.

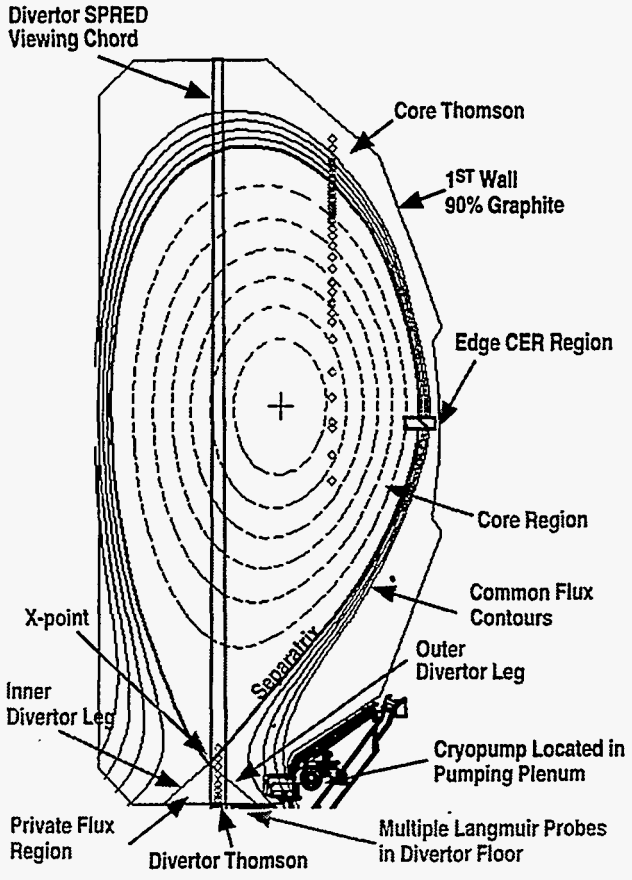

Fig. 1. A cross section of the DIII–D vacuum vessel with a flux contour plot of a typical lower single-null diverted plasma configuration is shown along with the locations of important divertor diagnostics. Also shown are the inner and outer divertor leg locations, the common and private flux regions, and the pumping plenum and cryo-pump.

The design of divertors for the next generation of tokamaks, in particular ITER, has led to the realization that the divertor's major role may be as much to protect the wall from the core plasma, as the reverse role it plays in today's machines. The high heat flux expected from ITER when operating in the ignited condition presents quite a problem to the engineering design of a robust divertor system. Using simple scaling relations for heat and particle flux derived from the "standard" operation of modern tokamak divertors, the ITER divertor is presented with conflicting design criteria. Without enhanced radiation, peak heat removal capability exceeding 25 MW/m^2 requires thin divertor strike plate components, while the expected first wall erosion rates and desired lifetime demand a minimum thickness for the strike plate. Thus, to achieve a robust and workable divertor for advanced tokamaks, today's experiments have begun to explore

operating modes of divertors that would lead to a reduction in peak heat flux in ITER to below 5 MW/m^2 while simultaneously reducing expected erosion rates [2,3].

Peak heat flux reduction has been obtained on a number of tokamaks in ELMing H–mode discharges (high confinement discharges with Edge Localized Modes) using: 1) strong deuterium gas puffing, 2) impurity gas puffing, and 3) a combination of both (see e.g. [4]). A time history of an ELMing H–mode discharge on DIII–D is shown in Fig. 2 where a steady deuterium fueling rate of 200 Torr·ℓ/s with matched exhaust rate is used to reduce the peak heat flux to the divertor by a factor of 5, with nearly steady conditions lasting for 2 s. In this case core Z_{eff} is maintained at about 1.8 with confinement improvement factor over ITER–89P L–mode scaling [5] of 1.7, closely approaching the ITER requirements. Substantial heat flux reduction has also been obtained on other major tokamaks using gas and impurity puffing. On ASDEX-Upgrade using a combination of gas fueling with exhaust and neon injection a clearly different mode of operation, labeled the CDH mode, is produced. During CDH–mode substantial radiation is produced in the edge of the core plasma [6,7]. In the DIII–D work discussed here the core radiation remains low. In this paper we will describe the ongoing work on the DIII–D tokamak to explore, document, and understand these modes of divertor operation, and the progress in developing detailed models used both to aid understanding and to provide predictive capability.

Simple 1D models of heat flow in ITER have indicated that the achievement of the necessary heat flux reduction will require a large radiation density over a significant fraction of the plasma volume in the outer divertor leg. The modeling also indicates that injected impurites, required to achieve the necessary radiation densities, must be concentrated in the divertor region in order to maintain low Z_{eff} in the core. Experiments on DIII–D, using the capability to simultaneously puff and exhaust deuterium gas, have demonstrated a high radiation density arising from the intrinsic deuterium and carbon over a large fraction of the plasma volume in the outer divertor leg. (The first wall of DIII–D is 90% graphite.) In other experiments, enrichment of injected neon and argon in the exhaust plenum region of the divertor has been demonstrated [8,9].

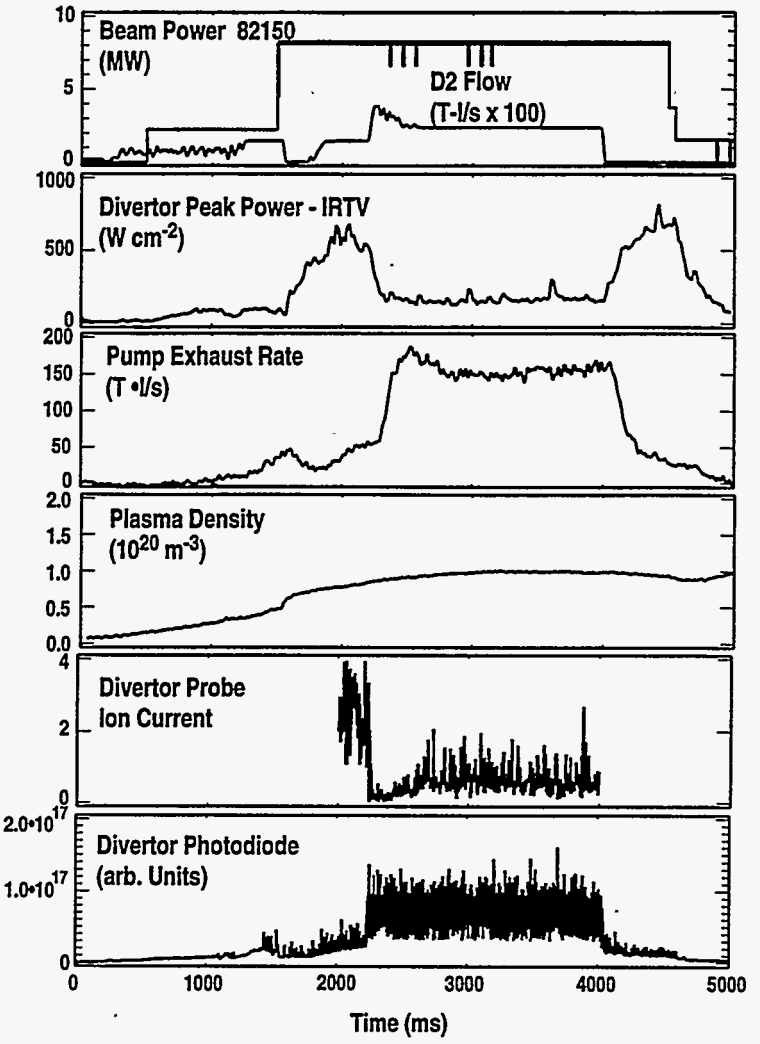

Fig. 2. The time history of several important discharge parameters from DIII–D discharge # 82150, where D_2 gas puffing combined deuterium exhaust using the cryo-pump was used to reduce the peak heat flux to the divertor by a factor of five compared to pre-puff conditions. The low heat flux condition was maintained in nearly steady-state for about 2 s.

2. THE DIVERTOR CHARACTERIZATION EXPERIMENTS ON DIII–D

The tokamak divertor is an inherently difficult plasma to diagnose. Strong spatial gradients exist in the plasma density and temperature, and in the impurity densities, ionization states, and line radiation. Thus to provide a detailed understanding, 2D profiles of most of these parameters are needed. During the past two years there has been a strong effort to put new diagnostics on DIII–D that provide effective 2D capabilities for many of these important plasma parameters. Key elements are a divertor Thomson scattering system, a fast plunging Langmuir probe, a 48 channel bolometer array, fixed Langmuir probes in the divertor strike plate, neutral deuterium and impurity gas pressure measurements, VUV and multichannel visible spectrometers, visible TV cameras with interference filters, and infrared cameras viewing the divertor strike plate. Figure 1 shows the location of some of these diagnostics on a cross section of the DIII–D tokamak along with a typical flux surface plot.

None of these diagnostics gives a direct 2D image of the measured parameter in the poloidal plane. Two-dimensional images of the total radiated power from the plasma are obtained using tomographic reconstructions of the 48 channel bolometric array [10]. Two-dimensional images of impurity and neutral deuterium line emission can be obtained from tomographic reconstructions of data from a tangentially viewing TV camera with visible interference filters [11].

To provide a 2D image of electron temperature and density from the divertor Thomson and plunging Langmuir probe, the plasma configuration must be swept in time across the diagnostic chords. Such sweeps are possible in DIII–D because of the open nature of the divertor region, and because of the versatile nature of the poloidal field coil set, power supplies, and control system. The divertor Thomson system obtains data at eight spatial locations along the vertical chord, ranging from 1 to 21 cm above the floor, at a 20 Hz repetition rate with a spatial resolution of about 1 cm

vertically and 5 mm radially and toroidally. The 2D "image" is reconstructed using the EFIT magnetic reconstruction code [12] to calculate the location of each divertor Thomson data point in Ψ and L_{pol} space, where Ψ is the poloidal flux value and L_{pol} is the poloidal length from the floor [13]. These points can then be remapped onto an R,Z plot at a particular time during the discharge.

Mappings of the divertor Thomson data for two DIII–D discharges, both with divertor sweeping, are shown in Fig. 3. Case A is a normal ELMing H–mode plasma with 4 MW of neutral beam heating. There is no gas fueling or impurity injection into this discharge. The divertor plasma is in the high recycling mode and fully attached to the strike plate. It is apparent from the figure that the electron density rises and the temperature drops somewhat as the plasma approaches the strike plate along a flux surface. The electron pressure, however, is approximately constant on a flux surface as is expected for the rapid parallel transport of the plasma along the open field lines. Case B of Fig. 3 is an ELMing H–mode plasma with heavy deuterium fueling at 6.5 MW of neutral beam heating. In this case, the plasma has made a transition to a partially detached state at the outer divertor (PDD). In this state, a region of enhanced radiation appears in the vicinity of the X-point, and the total radiated power is about 75% of the input power. Along flux surfaces just outside the separatrix, below the X-point the electron density is high, above 1×10^{20} m^{-3}, and nearly uniform along a flux surface, while the temperature has dropped to very low values, below 2 eV. At the plate, the electron pressure has dropped significantly below that on the same flux surface at the midplane. On flux surfaces further away from the separatrix, in the outer part of the scrape off layer, the plasma electron temperature at the strike plate remains well above 5 eV and the plasma is attached to the plate. In the detached region of the divertor near the separatrix there is a significant pressure drop between the midplane and strike plate, whereas in the outer SOL pressure balance remains (sometimes the pressure at the plate exceeds that at the midplane).

Reconstructions of data from bolometry and a tangentially viewing TV with a CIII filter during the attached and PDD phases of this discharge are shown in Fig. 4. During

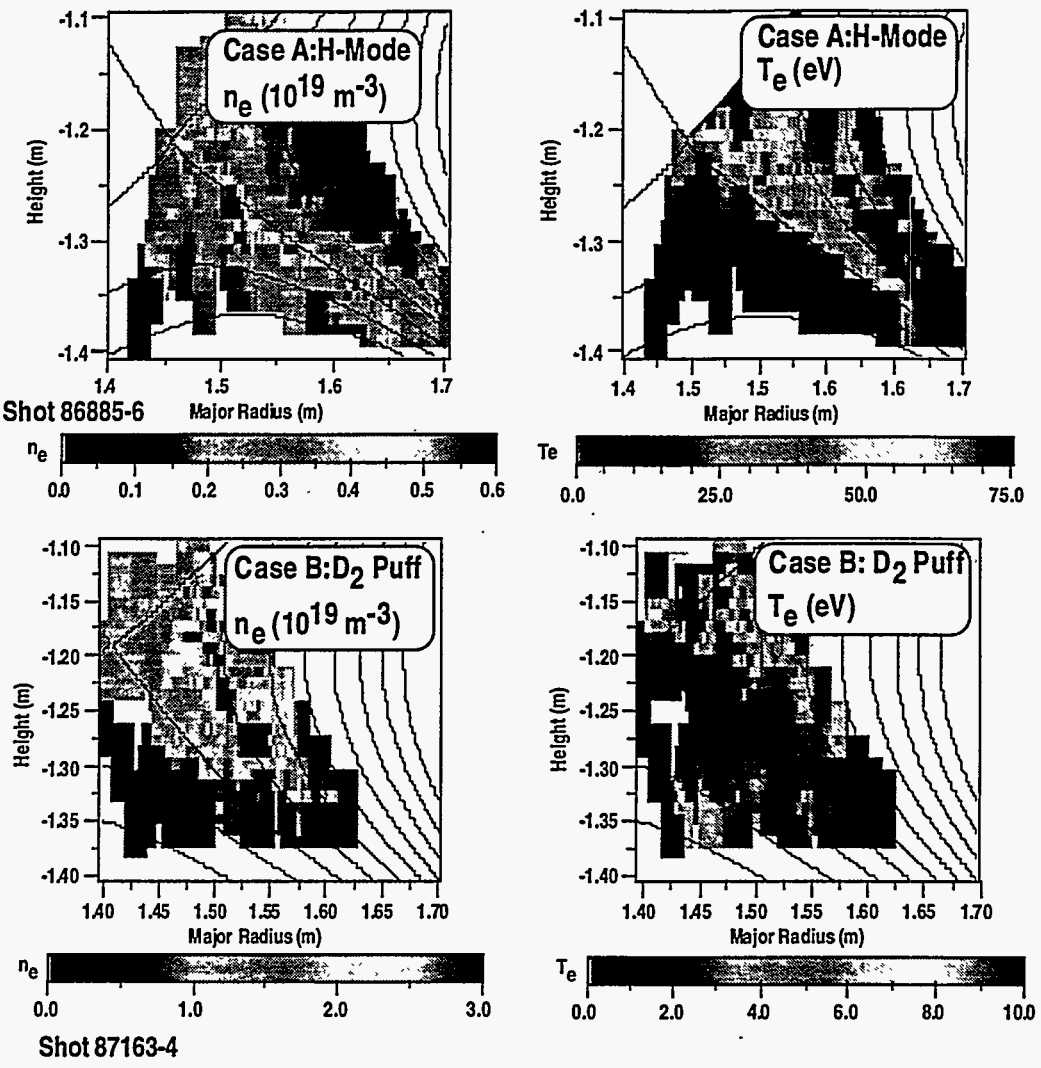

Fig. 3. False color images of the reconstructed divertor Thomson scattering data are shown for two discharge conditions: Case A, Standard ELMing H–mode operation and Case B, Partially detached divertor operation with a steady D_2 gas puff.

attached ELMing H–mode, the divertor radiation peaks along the inner leg, as does the CIII emission. D_α emission, not shown, also peaks along the inner leg, but nearer to the strike point than the CIII [14]. After the transition to the PDD state, the radiation increases over most of the divertor volume, and is seen to peak along the outer leg in the vicinity of the X-point. The CIII emission is seen to peak along the outer leg near the X-point. The peak in the D_α emission has also moved to the outer leg, residing just above the strike point.

Line emissivities of CII, CIII, CIV and Ly-β measured by the single chord VUV SPRED spectrographic instrument viewing the divertor from above (see Fig. 1) during a

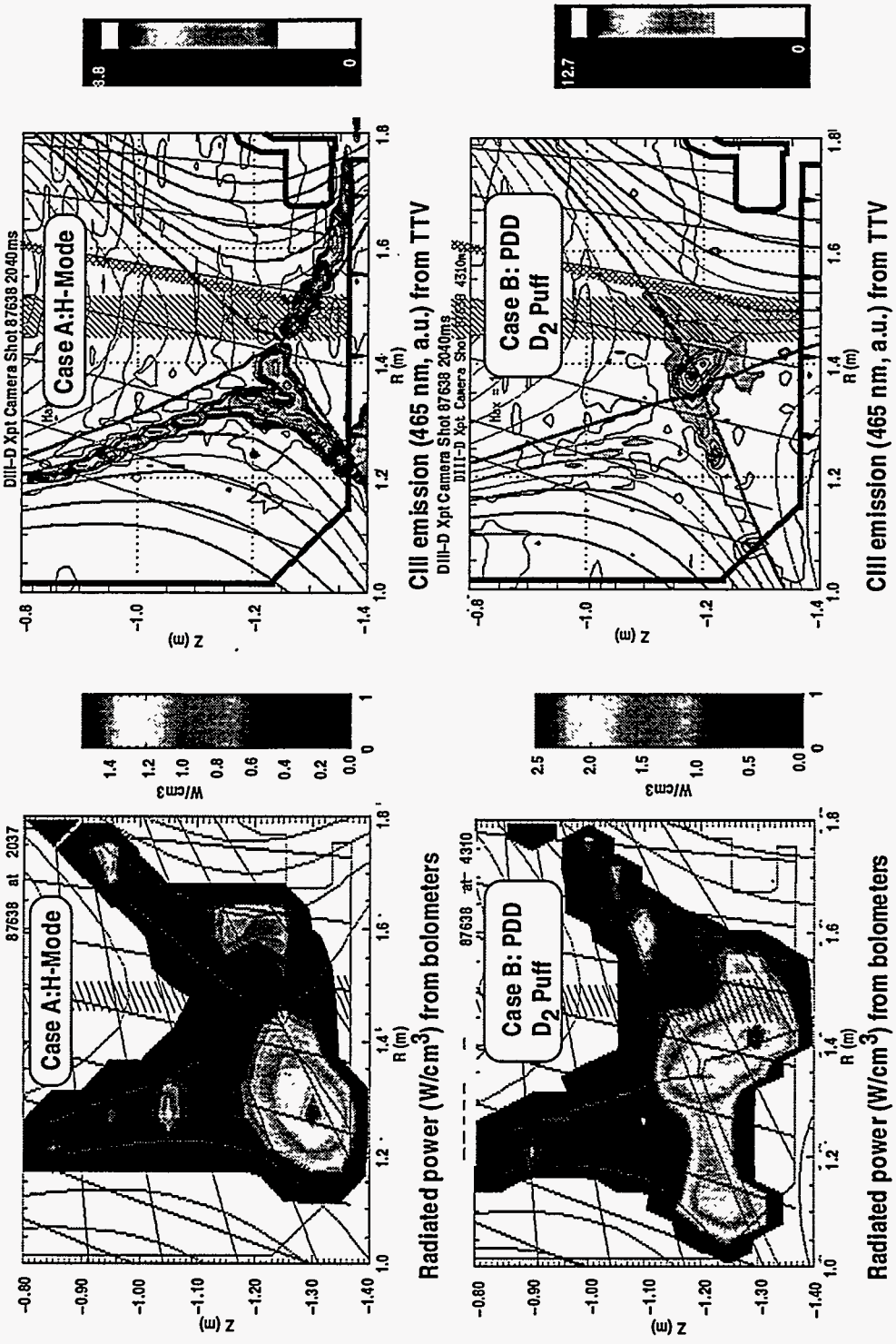

Fig. 4. Gray scale images of the reconstructed bolometry and tangential TV data showing the poloidal distributions of total radiated power and CII visible line emissivity for discharge conditions A and B in Fig. 3.

divertor sweep have been used to estimate the contribution of CIV and D to the total radiated power in the divertor [15, 16]. The measured emissivity of the CIV ion peaks when the viewing chord passes through the vicinity of the X-point, whereas the Ly-β peaks at the strike point, in qualitative agreement with the reconstructed visible camera views. The strongest line emission from carbon (CIV 155 nm) and deuterium (Ly-α 121 nm) are not measured by the spectrometer, however estimates of the local radiation from carbon and deuterium have been made from the measured VUV line emissivities. The reconstructed TV data indicates that the carbon radiation is highly localized. A local electron temperature in the vicinity of the strong carbon radiation is obtained from measured CIV line ratios that are temperature dependent. The obtained temperature, about 7 eV, is in reasonable agreement with the temperature measured with divertor Thomson scattering in the region of bright visible CIII emission. This temperature is then used, along with a detailed collisional-radiative model of carbon line emission and the measured line emissivities, to estimate the total radiated power for each carbon ionization state and deuterium. The results are shown in Fig. 5. CIV and D are seen to account for essentially all of the radiated power in the divertor. Near the X-point CIV heavily dominates, but near the strike point the CIV and D radiation are approximately equal. It appears that over the whole divertor, carbon is playing a dominant role in the radiation.

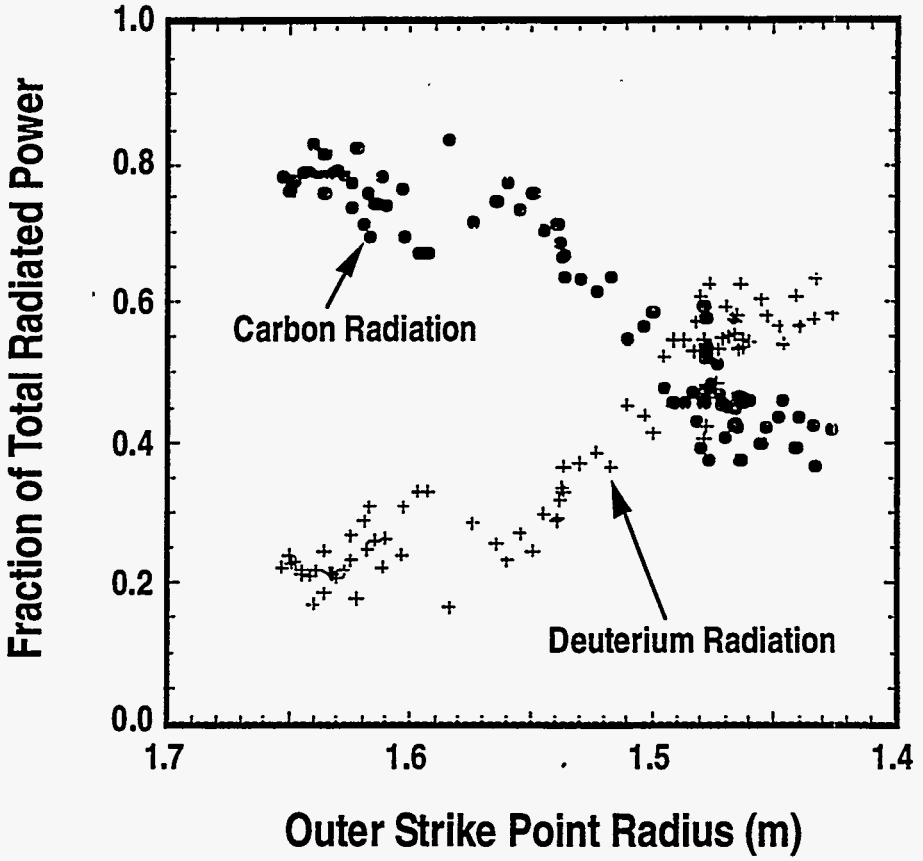

Fig. 5. The fraction of the total radiated power due to carbon and deuterium along a vertical chord viewing the divertor at R = 1.48 m is shown as a function of the location of the outer strike point during a strike point sweep. The line integrated radiated power due to carbon and deuterium are obtained from VUV spectroscopy as described in the text, and the total radiated power is obtained from bolometry.

3. TWO-DIMENSIONAL FLUID MODELING USING THE UEDGE CODE

UEDGE modeling of the detached plasma cases has shown the importance of neutral-ion momentum exchange in the high density region near the divertor plate, where the subsequent reduced flow velocities and low electron temperatures allow volume recombination to become important.[17] The UEDGE code is a 2D fluid model of the SOL and divertor plasma[18]. It has multi-species capability for ion fluids and uses classical parallel physics and anomalous perpendicular transport. The code has been used extensively to model attached ELMing H–mode plasmas in DIII–D, with good matching of midplane electron density and temperature profiles, and ion temperature profiles [19,20]. When impurity radiation is included, good agreement with divertor heat flux profiles and electron density and temperature profiles is also obtained. Recently the neutral fluid has been upgraded to a Navier-Stokes model permitting momentum transfer between the neutral and ion fluids [21].

In Fig. 6 UEDGE results for the electron density and temperature along the divertor Thomson chord for a case where the chord lies in the common flux region just outside the outer separatrix are compared to the measured values for a discharge similar to that shown in Fig. 3 Case B. In this case the full multi-species ion fluids version, which is only now being tested, was not used. Impurity radiation is included by assuming a constant fraction of 0.2% carbon ions in the plasma, and the radiative rate is non-coronal (corrected for charge exchange with neutral deuterium). For plasmas with power flux consistent with the experimental heating power, the UEDGE model does not achieve detachment on the outer divertor leg without impurity radiation. With the inclusion of carbon radiation, the temperature at the outer plate (and the inner plate not shown) is seen to fall to 1 eV and stays below 5 eV for a few cm away from the plate. The data indicate that T_e remains low further away from the plate. Only since the inclusion of the Navier-Stokes neutral fluid model has the code been able to produce a

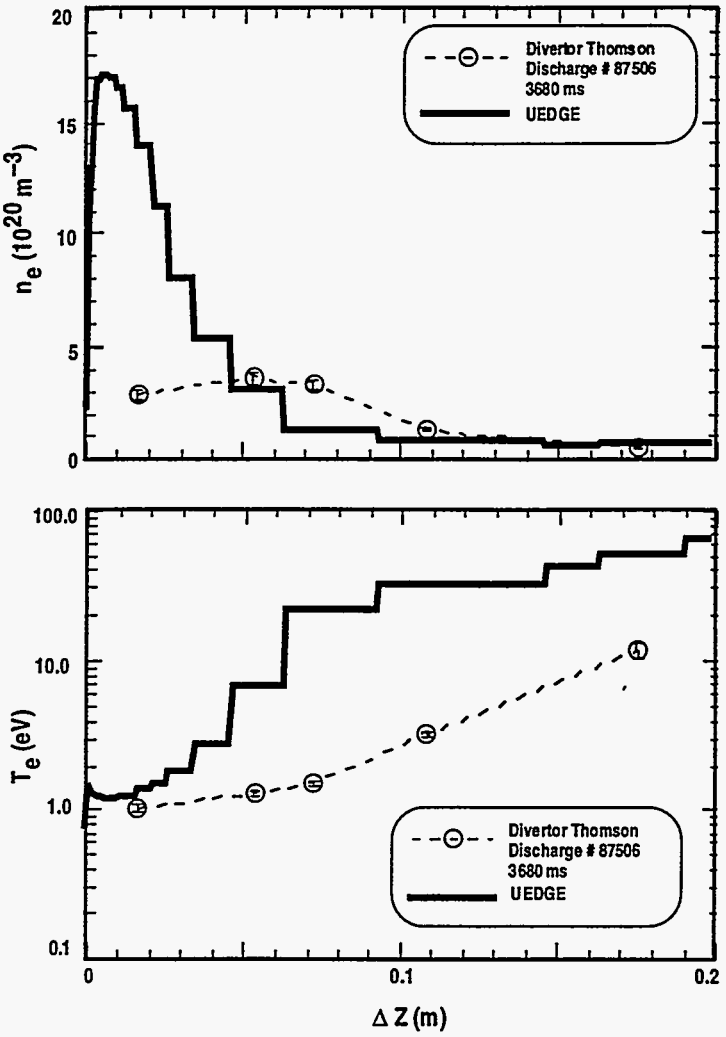

Fig. 6. Divertor Thomson data from a detached plasma is compared to the UEDGE simulation. Shown are the electron density and temperature along the divertor Thomson chord at a time when the chord is viewing the common flux region of the outer divertor leg.

cold high density region near the outer strike zone with the region of neutral ionization ($T_e > 5$ eV) pulled away from the plate when modeling these high powered discharges. The UEDGE model indicates (Fig. 7) the parallel flow of the ions in the cold plasma region is dropping to a low value. In this region, T_e has been reduced due to the carbon radiation, allowing the penetration of cold neutrals. The loss of parallel momentum results from charge exchange with these cold recycling neutrals. The ion flux to the plate is reduced due to a reduction in local re-ionization of recycled neutrals at $T_e <$ 5 eV, an effect seen in the Langmuir probe data (Fig. 2). The slow flow, along with the

high volume recombination rates resulting from the high-density, cold plasma, serve to further reduce the ion flux to the plate.

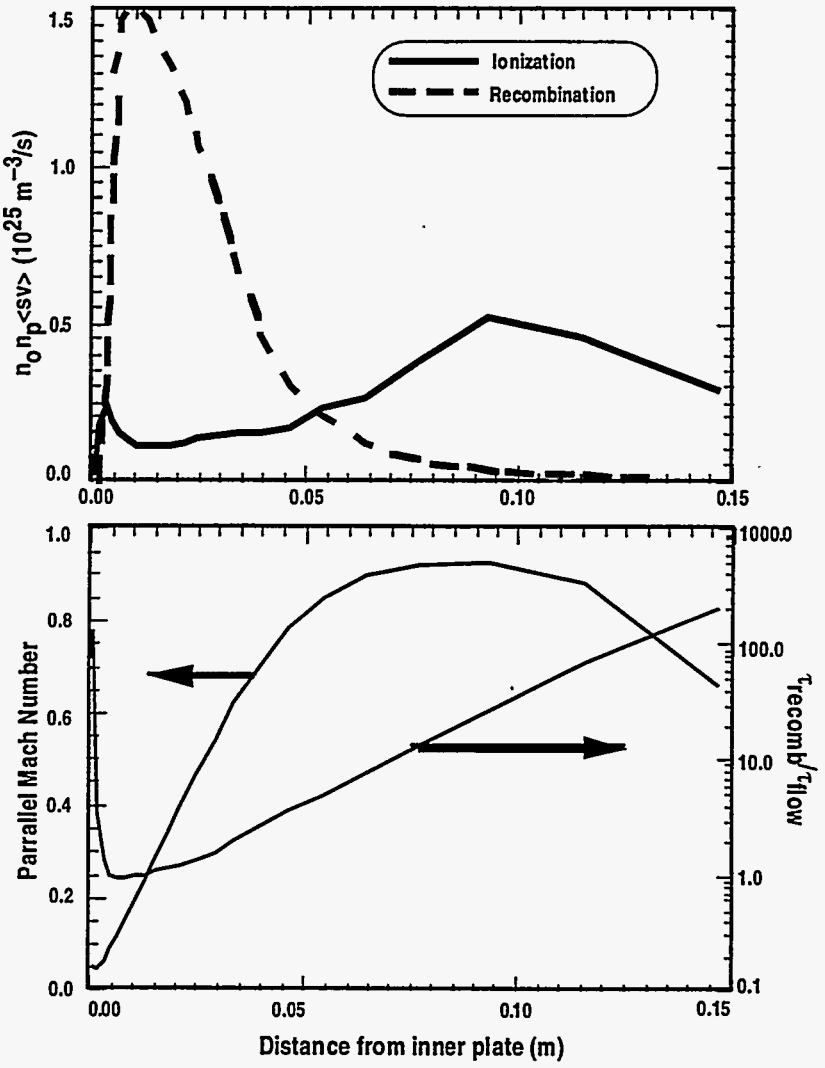

Fig. 7. The deuterium ionization and recombinations rates, the parallel flow (mach number), and the ratio of the recombination time to the flow time to reach the divertor plate are shown as a function of the poloidal distance to the plate for the UEDGE simulation of the detached condition shown in Fig. 6.

4. EXTENDED RADIATION ZONE

The current divertor design for ITER calls for increased divertor radiation to extend from the X-point to the divertor target with variation less than a factor of 6 in order to distribute power losses throughout the divertor structure. On DIII–D an extended divertor configuration with divertor poloidal length of ~50 cm was utilized to test the distribution of the increased divertor radiation during operation with reduced heat flux. With 10 MW of injected power in ELMing H–mode, deuterium gas was injected into the divertor at a rate of 190 Torr-ℓ/s to increase radiative losses and thereby decrease the divertor target heat flux. The radiative losses increased to 65% of the input power resulting in a decrease in the peak divertor heat flux of a factor of 3. The 2D distribution of radiative losses, plotted in Fig. 8, is measured by the bolometer array. The high X-point configuration allows 6 bolometer chords to pass though the outer divertor leg. Taking advantage of this spatial resolution, the outboard divertor radiation is seen to be uniform to within a factor of 2. Increased radiation in the periphery of the main plasma also contributed to the reduction of divertor heat flux. Further increased gas throughput results in radiation coalescing at the X-point inside the separatrix, the divertor plasma completely detaching from the divertor plate and L–mode confinement of the main plasma.

Gas puffing in this configuration results in a decrease in confinement. Before gas puffing the main plasma energy confinement is ~1.8 × ITER–89P scaling. With gas puffing the confinement progressively degrades to ~1.2 × ITER–89P. One possible explanation for the poorer confinement is the large empty volume in this configuration allowing transport of neutral gas from the divertor to the midplane. In fact, the midplane neutral pressure rises above 1 mTorr at this level of gas puffing. Baffling of the divertor in the future may help keep confinement high while still reducing the target plate heat flux [22].

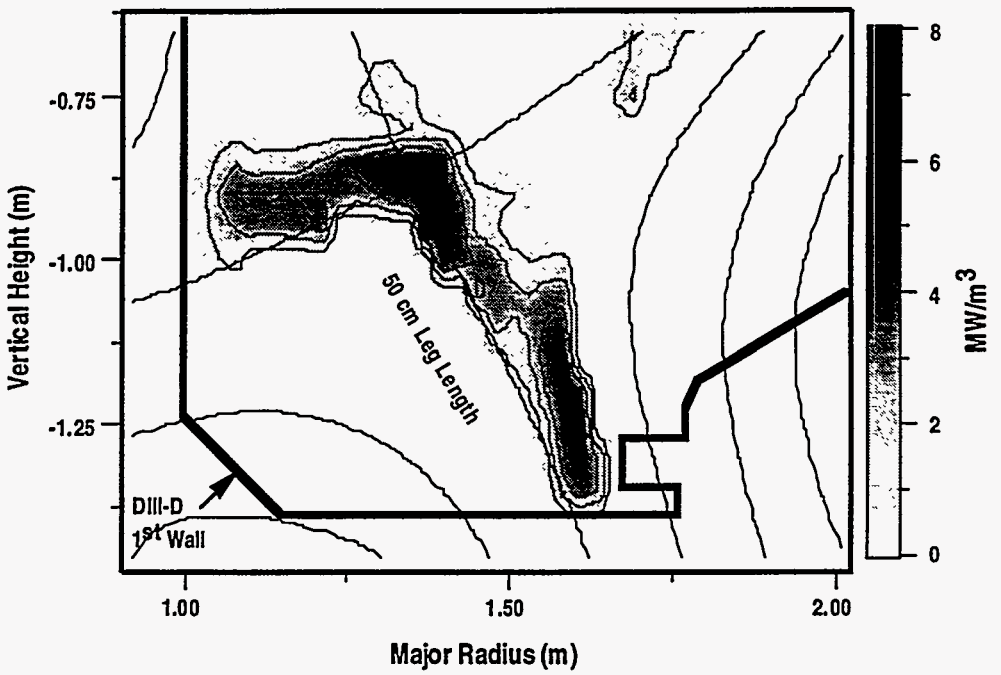

Fig. 8. Gray scale image of the poloidal distribution of radiated power along a 50 cm outer divertor leg obtained from reconstructed bolometry data. The extended region of high radiation is obtained during deuterium puffing with exhaust using the cryopump.

5. IMPURITY ENRICHMENT

In order to radiate sufficient power in the divertor of ITER, while maintaining acceptable levels of radiation and fuel dilution in the core plasma, it is necessary to enhance the impurity concentration in the divertor. One-dimensional models of impurity radiation have suggested that injected argon or neon used to enhance the radiation must have a higher concentration in the divertor than in the core, by approximately a factor of 3 [23,24]. Such enhanced divertor impurity concentration is termed "impurity enrichment". The enrichment factor is defined as the ratio of the divertor to core concentrations. The primary forces on impurity ions which act in the direction parallel to the magnetic field arise from collisional effects with the fuel ions [25]. A frictional force on the impurity ions arises from the flow of the fuel ion fluid, which is generally directed toward the strike plate and tends to keep the ions preferentially in the divertor. Working against the frictional force is the ion temperature gradient force, which tends to push the impurity ions to regions of hotter fuel ions, i.e. toward the core plasma. In the open divertor configuration of DIII–D, transport of recycled neutral impurities also will play a role in impurity enrichment. ELMs have also been seen to play an important role in the edge impurity transport [26].

Experiments have been run on DIII–D to test the ability to improve impurity enrichment by actively increasing SOL flow [8,9]. On DIII–D the divertor baffle and pump have been shown to allow significant throughput of fueling gas in a steady ELMing H–mode discharge. By fueling the discharge using gas puffing near the top of the vessel, and using the strong pumping divertor configuration, an enhancement of the parallel flow can be established in the outer SOL. Similar discharges can be run without enhancing the SOL flow by moving the gas fueling location to the private flux region of the divertor. Trace levels of neon or argon are puffed into the divertor region. Core impurity content is measured using charge exchange recombination spectroscopy

and the impurity content in the pumping plenum is measured using a modified Penning gauge which has been calibrated in-situ. At the present time, we have no direct measure of the impurity ion content in the divertor plasma, so here we present the results for the pumping plenum enrichment, which we call "exhaust enrichment". The results for neon and argon exhaust enrichment are summarized in Table I.

Table I: Comparison of measured exhaust enrichment for neon and argon for various cases of gas fueling location with pumping. The exhaust enrichment is defined as the ratio of the pumping plenum impurity concentration to the core impurity concentration at $\rho = 0.7$. Absolute enrichment factors for neon are quoted, however because of uncertainties in the charge exchange cross sections used to calculate core plasma argon concentrations, all argon enrichment factors are quoted relative to the divertor puffing location at 80 Torr-ℓ/s.

D_2 flow location	Top	Divertor	Top	Divertor
Flow (Torr-ℓ/s)	150	150	80	80
Line-averaged density	6.2×10^{19}	6.1×10^{19}	6.0×10^{19}	6.1×10^{19}
Baffle pressure (mTorr)	4.0	3.5	1.6	1.5
ELM frequency (Hz)	60	55	60	55
Neon enrichment	1.4	1.0	1.2	1.0
Argon enrichment (relative)†	6.9	2.2	1.7	1.0

†Normalized to enrichment in 80 Torr-ℓ/s, divertor fueling case

Comparing the cases for top fueling and divertor fueling at similar ELM frequency, it is clear that SOL flow does provide an enhancement of neon enrichment. Comparing cases (not shown) for similar flow with different ELM frequency indicates that ELMs are also playing an important role [8]. Similar data for helium enrichment yield enrichment factors lower than those seen for neon. The dependence on the impurity species may result from the significant changes in the ionization path length, which is dropping as the impurity Z increases. Studies of the dependence of exhaust enrichment on fuel throughput on ASDEX-Upgrade [27] during detached divertor operation (CDH–mode) with Type 3 ELMs has indicated no dependence on SOL flow, but a significant dependence on divertor density. The enrichment factor for neon was

observed to increase with increasing density, or equivalently shorter ionization length. While the lack of dependence on flow appears to be in conflict with the DIII–D results, the different operating conditions and divertor geometries are likely to affect the complex balance of the various processes involved in divertor impurity transport. Further work is needed to help elucidate the apparent discrepancy in these data.

6. DIVERTOR PUMPING OF HELIUM

To maintain ignition in a burning tokamak, the helium ash produced in the d,t fusion process must be exhausted at a rate sufficiently high to prevent excessive fuel dilution. Studies have shown that ignition can be maintained if the time constant for helium ash removal $\left(\tau^*_{He}\right)$ is less than 15 energy confinement times (τ_E)[28]. Exhaust of helium ash has been demonstrated on DIII–D in ELMing H–mode discharges, mimicing a central source of helium using 75 keV neutral helium beam injection [29]. The ratio τ^*_{He}/τ_E was determined to be approximately 8, consistant with previous measurements using helium gas puffing as the source[30]. Helium exhaust studies on ASDEX Upgrade during CDH operation using helium gas puffing as the source have demonstrated τ^*_{He}/τ_E of as low as 7 [31,32]. On both tokamaks, the helium is observed to be somewhat diluted in the exhaust plenum, compared to the core plasma, with exhaust enrichment factors in the range of 0.3 to 0.4. These values are well in excess of the 0.2 value used for the ITER design.

7. SUMMARY

Experiments on DIII–D designed to characterize highly radiating divertor plasmas produced by heavy gas fueling have successfully been carried out. In these partially detached plasmas in the common flux region near the separatrix, a region of cold ($T_e <$ 2 eV), dense ($n_e > 1 \times 20$ m^{-3}) plasma extends from the outer divertor strike point to near the X-point. Further out from the separatrix, the plasma remains attached, with $T_e > 5$ eV. Visible and VUV spectroscopy of the divertor indicates that carbon dominates the radiation in the outer leg of the divertor except near the strike point, where deuterium and carbon are both significant radiators.

The partially detached condition has been simulated using the 2D fluid model, UEDGE. The modeling indicates the importance of radiative cooling and charge exchange momentum loss. In the cold, dense region of the plasma, volume recombination is important for reducing the ion flux to the plate.

Using a 50 cm outer divertor leg length, a highly radiating region of plasma along the outer divertor leg from the X-point to the strike point has been produced. Bolometry shows that the radiation density in this region is constant to within a factor of 2. Such an extended, uniform zone of radiation is planned for the ITER divertor.

The ability to enhance the exhaust enrichment of injected neon and argon using gas fueling and strong divertor pumping to increase SOL flow has been demonstrated. Using a steady particle throughput of 150 Torr-ℓ/s with fueling at the top of the plasma, an enrichment factor increase of 40% for neon was obtained over a case with 80 Torr-ℓ/s fueling in the divertor. Using trace argon injection, an enrichment factor increase of over 6 is achieved between the same two cases. If this exhaust enrichment is reflective of divertor enrichment, which was not measured in the DIII–D experiments, then flow enhancement may be useful in ITER to meet the required divertor radiation and core Z_{eff}.

Exhaust of helium ash at rates exceeding requirements for maintaining ignition in a tokamak has been demonstrated in diverted tokamaks operating in ELMing H–mode with a centralized source of helium and in highly radiating detached divertor operation. The exhaust enrichment measured for helium in these experiments exceeds that presently used in the ITER design.

REFERENCES

[1] The ASDEX Team, Nucl. Fusion **29**, 1959 (1989).

[2] G. Janeschitz, "ITER Divertor Design Document," WBS1.7 (1995).

[3] G. Janeschitz, et al., "The ITER Divertor Concept," J. Nucl. Mater. **220–222**, 73 (1995).

[4] T.W. Petrie, et al., "Radiative Divertor Experiments in DIII–D With D_2 Injection," J. Nucl. Mater. **196-198**, 848 (1992).

[5] P.N. Yushmanov, et al., Nucl. Fusion **30**, 1999 (1990).

[6] O. Gruber, A. Kallenabch, M. Kaufmann, et al., Phys. Rev. Lett. **74**, 4217 (1995).

[7] A. Kallenbach, R. Dux, V. Mertens, et al., Nucl. Fusion **35**, 1231 (1995).

[8] M.J. Schaffer, M.R. Wade, R. Maingi, et al., "Direct Measurement of Divertor Neon Enrichment in DIII–D," in Proc. of 12th Conf. Plasma Surface Interactions, St. Raphael, France 1996, to be published in the J. of Nucl. Mater.

[9] M.J. Schaffer, et al., "Impurity Reduction During Puff and Pump Experiments on DIII–D," Nucl. Fusion **35**, 1000 (1995).

[10] A.W. Leonard, et al., Rev. Sci. Instrum. **66**, 1201 (1995).

[11] M.E. Fenstermacher, et al., "A Tangentially Viewing Visible TV system for the DIII–D Divertor," to be published in Rev. Sci. Instrum.

[12] L. Lao, et al., Nucl. Fusion **30**, 1035 (1990).

[13] S.L. Allen, D.N. Hill, T.N. Carlstrom, et al., "Measurements of T_e and n_e With Divertor Thomson Scattering in Radiative Divertor Discharges on DIII–D," in Proc. of 12th Conf. Plasma Surface Interactions, St. Raphael, France 1996, to be published in the J. Nucl. Mater.

[14] M.E. Fenstermacher, R.D. Wood, S.L. Allen, et al., "Comprehensive 2D Measurements of Radiative Divertor Plasmas in DIII–D," in Proc. of 12th Conf.

Plasma Surface Interactions, St. Raphael, France 1996, to be published in the J. Nucl. Mater.

[15] R.D. Wood, R.C. Isler, S.L. Allen, *et al.*, "Measurement Of Divertor Impurity Concentrations on DIII–D," in Proc. of the 23rd European Physical Society Conference on Controlled Fusion and Plasma Physics, Kiev, Ukraine, 1996.

[16] R.C. Isler, et al., "Spectroscpic Characterization of the DIII–D Divertor," to be submitted to Physics of Plasmas.

[17] G.D. Porter, et al., "Divertor Characterization Experiments and Modeling in DIII–D," in Proc. of the 23rd European Physical Society Conference on Controlled Fusion and Plasma Physics, Kiev, Ukraine, 1996.

[18] T. Rognlien, et al., "A Fully Implicit, Time Dependent 2D Fluid Code for Modeling Tokamak Edge Plasmas," J. Nucl. Mater. **196-198**, 347 (1992).

[19] M.E. Fenstermacher, et al., "UEDGE and DEGAS Modeling of the DIII–D Scrape-off Layer Plasma," J. Nucl. Mater. **220-222**, 330 (1995).

[20] G.D. Porter, et al., "Analysis of Particle Flow in the DIII–D SOL and Divertor," in Proc. of the 19th European Physics Society, 1995, Bournemouth, England.

[21] G.D. Porter, *et al.*, "Simulation of Experimentally Achieved DIII–D Detached Plasmas using the UEDGE Code," Phys. Plasmas **3**, 1967 (1996).

[22] S.L. Allen, et al., J. Nucl. Mater. **220-222**, 336 (1995).

[23] D. Post, et al., J. Nucl. Mater. **220-222**, 1014 (1995)

[24] M.A. Mahdavi, et al., "Stability of a Radiative Mantle in ITER," Proc. of 12th Conf. Plasma Surface Interactions, St. Raphael, France 1996, to be published in the J. Nucl. Mater.

[25] J. Neuhauser, et al., Nucl. Fusion **24**, 39 (1984).

[26] M. Perry et al., Nucl. Fusion **4**, 710 (1980).

[27] H.-S. Bosch, et al., "Invariance of Divertor Retention on External Particle Flow in Detached ASDEX Upgrade Discharges," Phys. Rev. Lett. **76**, 2499 (1996).

[28] D. Reiter, et al., Nucl. Fusion **30**, 2141 (1990).

[29] M.R. Wade, et al., Phys. Rev. Lett. **74**, 2702 (1995).

[30] M.R. Wade, et al., Phys. Plasmas **2**, 2357 (1995).

[31] H.-S. Bosch, et al., "Particle Exhaust in Radiative Divertor Experiments," Proc. of 12th Conf. Plasma Surface Interactions, St. Raphael, France 1996, to be published in the J. Nucl. Mater.

[32] H.-S. Bosch, et al., "Helium Transport and Exhaust Studies in ASDEX Upgrade," Proc. of 3rd International IEA Workshop on Helium Transport and Exhaust, Charleston, South Carolina, September 1995, to be published.

ACKNOWLEDGMENT

This is a report of work supported by the U.S. Department of Energy under Contract Nos. DE-AC03-89ER51114, W-7405-ENG-48, DE-AC04-94AL85000, DE-AC05-96OR22464, and Grant Nos. DE-FG03-95ER54294 and DE-FG03-86ER53266.